International Journal of Smart Energy Technology and Environmental Engineering
Volume 2, Issue 2, September 2023
http://globalpublisher.org/journals-1007/
DOI: 10.52547/setee.2.2.144

Creating the applicability range of hydrodynamics in high energy collisions

Reza Khaki[1,*], Akbar malayeri[1], Amir bazovarz[1], Shahrokh abdolkhani[1]
1- Department of Mechanical Engineering, South Branch, Islamic Azad University, Tehran, Iran
*Corresponding Author: r_khaki@vu.iust.ac.ir

ABSTRACT

We simulate the spatio-temporal dynamics of high-energy collisions based on a microscopic kinetic description in the coherent-time approximation, to determine the applicability of an effective description in relativistic viscous hydrodynamics.
We find that hydrodynamics gives a quantitatively accurate description of the collective flow when the mean inverse Reynolds number 〖Re〗^(-1) is sufficiently small and the early pre-equilibrium state is specifically considered. has been From now on, we discuss the implications of our findings for the applicability or nonapplicability of hydrodynamics in proton-proton, proton-nucleus, and nucleus-light collisions.

Keywords*:* Reynolds number, nucleus-light, hydrodynamics

1. Introduction

Relativistic high-energy ion collisions probe the behavior of strongly interacting matter under extreme conditions. One of the main goals of these experiments is to determine the properties of quark-gluon-plasma, a new phase of nonconfined highly interacting matter. . The emergence of collective phenomena in such collisions has been successfully described using relativistic viscous hydrodynamics, which forms the central part of multi-stage evolutionary models in modern simulation frameworks.[1]

Despite the widespread phenomenological success, it is important to remember that viscous relativistic hydrodynamics with its structure is an effective macroscopic description of the basis of microscopic quantum chromodynamics theory, which aims to describe the long-time and long-wavelength behavior of near-equilibrium quantum chromodynamics. Consequently, the applicability of hydrodynamics requires the separation of the time scale and length scale of the dynamics of microscopic alternatives and those of the macroscopic dynamics of the system integrally and several degrees of quark-gluon-plasma equilibrium, both of which occur in high-energy ion collisions. They are not necessarily realized. [2]

While for high-numbered events we can see the system rapidly reaching equilibrium, establishing the time scale of this process with practical motivations has so far been largely

speculative. In recent years, the observation of collective flow even in small colliding systems, which were traditionally considered too dilute to allow quark-gluon-plasma formation, has challenged the model of hydrodynamics. While considerable progress has been made in understanding the origin and applicability of hydrodynamic behavior in the simple case of Bjorken flow. Despite several considerable efforts, the basic question under which conditions viscous hydrodynamics provides us with an accurate and reliable description of the complex space-time dynamics of real-world collisions remains largely unanswered [3]. Here, we use a microscopic description in relativistic kinetic theory to determine the applicability of viscous hydrodynamics in high energy collisions. Starting from a non-equilibrium steady state immediately after the collision, we find that even in the limit of very large interaction forces, the early pre-equilibrium dynamics can never be described by ordinary viscous hydrodynamics, which on the observed cases can It affects with a small percentage. Subsequently, for sufficiently large systems, the fluid approaches equilibrium before transverse expansion and the development of transverse anisotropic flow can be described macroscopically using viscous relativistic hydrodynamics. Adapting the non-equilibrium kinetic description to relativistic viscous hydrodynamics, we determine a fundamental inverse Reynolds number 〖Re〗_c^(-1) based on which hydrodynamics can describe the quark-gluon-plasma space-time dynamics, which includes the development And the anisotropic transverse flow expansion is also slightly accurate. Conversely, for small or high viscosity systems, the system remains out of equilibrium in the evolution interval, and we evaluate when the conditions for the applicability of viscous hydrodynamics are met. become a function of shear viscosity relative to entropy density, ground state energy density, and system size, and thus result in the limits of hydrodynamic applicability in small systems [4].

Since the reasons for hydrodynamic failure in the early state can be understood and effectively solved by Bjorken flow dynamics, we decide on another method that allows us to start the hydrodynamic simulation immediately after the collision, at time zero. , which is by compensating the misdescription at initial times by rescaling the initial conditions. Here, we focus on relevant phenomenological findings [5].

2. Implementation of kinetic theory

To study the evolution of the microscopic space-time dynamics, we use the Boltzmann equation in the relaxation time approximation.

$$p^{\mu}\partial_{\mu}f(x,p) = -\frac{u^{\mu}(x)p_{\mu}}{\tau_R(x)}[f(x,p) - f_{\mathrm{eq}}(x,p)] \tag{1}$$

Equation 1 above, with a coherent relaxation time as Equation 2 below

$$\tau_R(x) = [(\eta/s)/5T(x)] \tag{2}$$

Equilibrium distribution f_eq with temperature T(x) and flow velocity u^μ (x), obtained through Landau adaptation u_μ T^μν=εu^ν, where we have ε=aT^4 and represents the density energy, a=(ν_eff π^2)/30 with ν_eff is equal to the effective number of degrees of freedom (bosonic) and is equal to the energy-momentum tensor.

$$T^{\mu\nu}(x) = \int_p p^\mu p^\nu f(x.p) \tag{3}$$

Due to the special simplicity of this microscopic theory, the space-time differences of the collision dynamics for a fixed initial energy density profile (ϵτ)_0 (X_⊥)
It depends only on a dimensionless darkness parameter [6].

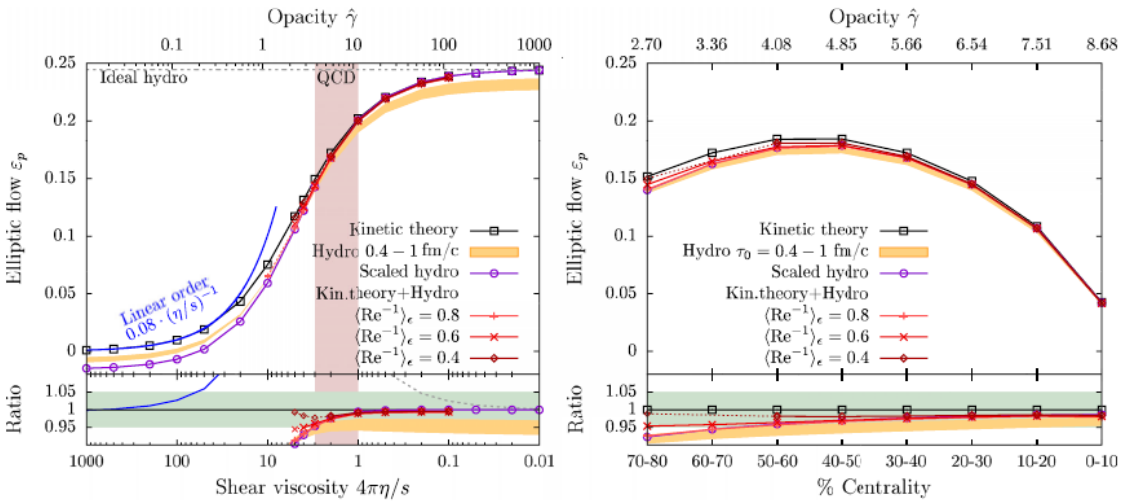

FIG. 1. Variations of the elliptic flow (left) as a function of the shear viscosity to entropy density ratio η=s for 30%–40% Pb þ Pb collisions and (right) as a function of collision centrality for fixed η=s ¼ 2=4π. Simulations in kinetic theory (black squares) are compared to ideal (gray dashed) and viscous hydrodynamics (purple circles) as well as hybrid simulations (red pluses, crosses, and diamonds) matching kinetic theory to hydrodynamics at different values of the average inverse Reynolds number Re−1 . Bands also show the results for naive hydrodynamics simulations with varying initialization times τ0 ¼ 0.4–1.0 fm=c. Semianalytic results from a leading order opacity expansion are shown as a blue curve in the left panel.

Elliptical flow changes (left side) are plotted as a function of shear viscosity to entropy density ratio and on the right side as a function of collision centrality.

$$\hat{\gamma} = \frac{1}{5\eta/s}\left(\frac{R}{\pi a}\frac{dE_\perp^0}{d\eta}\right)^{1/4} \tag{4}$$

which is considered for changes in shear viscosity in relation to entropy density, and initial energy per unit of speed, system size [7].

To reach the optimal collision geometry, we focus on the collision in the Large Hadron Collider and examine a profile of the average ground state energy density obtained from the saturation model, and by changing the shear viscosity in proportion to the entropy density and the centrality of the collision to We review and evaluate the shutdown dependency. We quantify the development of transverse anisotropic flow in the form of sentences of elliptic energy flow.

$$\varepsilon_p = \frac{\int_{\mathbf{x}_\perp} T_{xx}(\mathbf{x}_\perp) - T_{yy}(\mathbf{x}_\perp) + 2iT_{xy}(\mathbf{x}_\perp)}{\int_{\mathbf{x}_\perp} T_{xx}(\mathbf{x}_\perp) + T_{yy}(\mathbf{x}_\perp)} \tag{5}$$

which we find directly from the energy-momentum tensor, and thus remove the uncertainties related to the hadronization process. Microscopic simulations in kinetic theory are compared with macroscopic description of relativistic hydrodynamics [9].

3. Collective flow and the applicability of hydrodynamics

To assess the applicability of the hydrodynamic description, we compare the results with the microscopic simulations in the kinetic theory of Fig. 1. We present the final results for elliptical energy flow collisions as a function of mid-center collisions in the left figure [10]. and for real values as a function of centrality in the figure on the right. When starting with the kinetic theory results, one immediately notices a significant damping (quenching) dependence of the final state impulse response relative to the ground state geometry. In the low quench limit, the final anisotropic Nadir current is generated by the final state Nadir interaction and can be well described by the leading quench expansion order, as shown by the blue line. Subsequently, for smaller values the anisotropic current response increases monotonically as a function of the quench and finally saturates at large quenches. It is interesting to observe that the predicted values for quantum chromodynamics lie in the region where the final state response exhibits a significant dependence on quenching, where the viscosity changes to Fifty percent size results in anisotropic current changes of about 15%. Now that we have established a foundation based on kinetic theory, we can compare the microscopic results with those obtained using the hydrodynamic description. Clearly, the first thing to notice is that in the limit of infinite quenches, the results of the kinetic theory converge to ideal hydrodynamics, indicated by the horizontal line. As we will now explain, this seemingly self-evident agreement is actually rather trivial. Due to the rapid longitudinal expansion, the system is initially unable to withstand significant longitudinal strain, which is only developed during the time course of the thermalization process. Based on the coherent behavior of the system, this pressure isotropy occurs faster in the hotter regions of the plasma than in the colder regions. Since the system works against longitudinal expansion. The pre-equilibrium evolution of longitudinal pressure affects the evolution of energy density and leads to the phenomenon of inhomogeneous longitudinal cooling. where the hotter plasma regions begin to cool faster than the colder plasma regions, thus leading to a small but non-negligible change in the geometry of the energy density profile even before the onset of anisotropic transverse expansion [11].

On the contrary, in ideal hydrodynamics the system is always assumed to be in isotropic local thermal equilibrium and there is no inhomogeneous longitudinal cooling effect. In order to recover the correspondence with the ideal hydrodynamics in the limit of infinite quenches, it is actually necessary to simulate the ideal hydrodynamics with the initial balanced energy density profile. While inhomogeneous longitudinal cooling is absent in ideal hydrodynamics, viscous hydrodynamics misrepresents this effect because it generally has a negative longitudinal pressure at very early times. Similar to the case of ideal hydrodynamics, this effect can be compensated for by changing the local scale of the initial energy density profile. In particular, we want that under the evolution of the Bjorken flow, the late behavior of the energy density is consistent between hydrodynamics and kinetic theory. Mathematically, we use the absorbing solution for the non-equilibrium evolution of the energy density[12].

$$\tau^{4/3}\epsilon = \frac{\tau_0^{4/3}\epsilon_0}{\mathcal{E}(\tilde{w}_0)}\mathcal{E}(\tilde{w}) \tag{6}$$

where epsilon is a global function that is the only isomorphic scaling variable with its environmental behavior at initial and final times defined by the following relation

$$\mathcal{E}(\tilde{w} \ll 1) = C_{\infty}^{-1}\tilde{w}^{\gamma}, \qquad \mathcal{E}(\tilde{w} \gg 1) = 1 - \frac{1}{4\pi\tilde{w}} \tag{7}$$

The coefficients describing the longitudinal cooling at early times have different values in the kinetic theory, taking advantage of the fact that the kinetic theory is constant at early times, then we show the energy density in hydrodynamics as follows

$$\epsilon_0^{\text{hydro}}(\mathbf{x}_\perp) = \left[\left(\frac{4\pi\eta/s}{\tau_0}a^{\frac{1}{4}}\right)^{\frac{1}{2}\frac{9\gamma}{8}}\left(\frac{C_\infty^{\text{RTA}}}{C_\infty^{\text{hydro}}}\right)^{9/8}\frac{(\epsilon\tau)_0(\mathbf{x}_\perp)}{\tau_0}\right]^{\frac{8/9}{1-\gamma/4}} \tag{8}$$

By performing local rescaling, viscous hydrodynamics can be quantified at arbitrary initial times, providing an accurate description of the anisotropic flow up to the extent of blackouts, as seen in the purple curve in Figure 1 [13].
Finally, we note that if the pre-equilibrium region is completely neglected and the hydrodynamic simulations are simply started with the initial energy density profile at a suitable time constant, the above effects and the absence of the pre-flow lead to significant deviations even in the limit of very large quenches. . In all cases, similar results can be obtained for radial flow development and plasma cooling.

4. Critical inverse Reynolds number

Due to the aforementioned sensitivities associated with the pre-equilibrium stage, another suitable alternative is to use a kinetic description at early times when the system is far from equilibrium and to switch to a macroscopic description only when the system is sufficiently close to equilibrium. Thermal is close, so that hydrodynamics is applicable. While in phenomenological studies the time scale to start the hydrodynamic simulation is usually chosen to be one femtometer/s, a more complete physical choice can be made by monitoring the amount of non-equilibrium corrections, as characterized by the (average) inverse Reynolds number. achieved [16].

$$\text{Re}^{-1} = \left(\frac{6\pi^{\mu\nu}\pi_{\mu\nu}}{\epsilon^2}\right)^{1/2} \tag{9}$$

where is the shear stress tensor of the non-equilibrium part. By moving from kinetic theory to hydrodynamics at different values of the inverse Reynolds number, we can then deduce what degree of balance is required for hydrodynamics to provide an accurate description of space-time dynamics [18]. The simulation results for the hybrid simulation using kinetic theory and hydrodynamics are also presented in Figure 1 and are in very good agreement with microscopic calculations from kinetic theory at large quenches. It is noteworthy, when comparing the results obtained with the change At different Reynolds numbers, it is observed that the agreement

between the kinetic theory and hybrid simulations improves significantly as the inverse Reynolds number decreases at the change point.

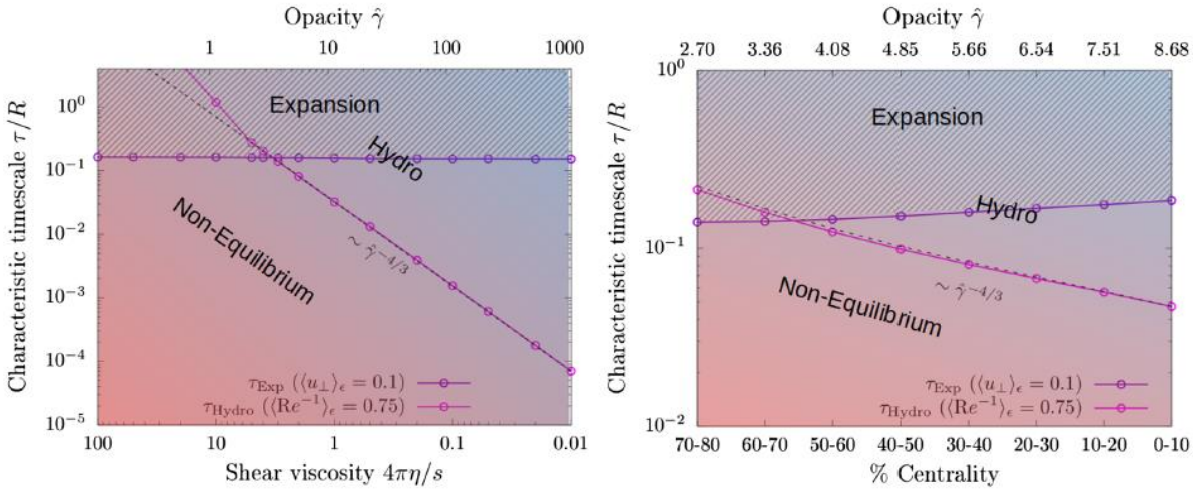

FIG. 2. Characteristic timescales for the onset of the transverse expansion τexp and the onset of hydrodynamic behavior τhydro (left) as a function of η=s for 30%–40% Pb þ Pb collisions and (right) as a function of collision centrality for fixed 4πη=s ¼ 2. Dashed lines indicate the γˆ−4=3 estimate for the transition between nonequilibrium and hydrodynamic behavior in Eq. (8). Below opacities γˆ ≃ 3–4, the transverse expansion sets in while the system is significantly out of equilibrium and hydrodynamics is unable to accurately describe the transverse expansion of the system.

Typical time scales for onset of transverse expansion and onset of hydrodynamic behavior (left) as a function of collisions and (right) as a function of collision centrality for dashed lines[20]
In particular, a sufficiently small inverse Reynolds number is obtained only after a long period of evolution in the kinetic theory. To recognize this behavior, the curves for which the time change exceeds five tenths are shown in Fig. 1 with The dashed lines show that, finally, for very large viscosities or very peripheral collisions, the inverse Reynolds number may never reach the desired value throughout the evolution of the system [19].

5. Scope of application of hydrodynamics

Based on the observation that a critical inverse Reynolds number of 0.75 is required for application of viscous hydrodynamics, we can immediately rule out the existence of a hydrodynamic description at small quenches, where the system remains significantly out of equilibrium throughout its evolution. remains and this threshold never occurs. However, at smaller viscosities, the above threshold may be reached at a very early time or at a relatively late time, and the question of whether or not hydrodynamics is applicable becomes a more sensitive issue. Hence, to quantify whether hydrodynamics provides a meaningful and accurate description of the space-time dynamics of high-energy collisions, we will compare the time scale for equilibration of the system, at the onset of transverse expansion, with the mean velocity The transverse flow becomes 0.1 times the speed of light, as shown in Figure 2. Irrespective of quenching, the transverse expansion spans the time scales, albeit with some dependence on the initial energy density profile, as can be seen from the central dependence of the curve in the right image [22]. Conversely, the time scale for hydrodynamic application shows a strong turbidity dependence that can be quantified semi-empirically. The time scale

for hydrodynamic application shows a strong dependence on quenching, which can be semi-empirically calculated quantitatively in the form of the relation below.

$$\tau_{\text{hydro}}/R \approx 1.53\hat{\gamma}^{-4/3}[(\text{Re}_c^{-1})^{-3/2} - 1.21(\text{Re}_c^{-1})^{0.7}] \tag{10}$$

As shown by the dashed line in Figure 2. By comparing the different curves in Figure 2, we conclude that for shutdowns

$$\hat{\gamma} \gtrsim 3\text{–}4 \tag{11}$$

which corresponds to collisions, the system is well equilibrated before the onset of transverse expansion, so that viscous hydrodynamics provides a meaningful and accurate description of the development of the transverse (anisotropic) flow. Conversely, hydrodynamics is not applicable when the system remains out of equilibrium during transverse expansion, and instead a true non-equilibrium description is required[26].

6. Conclusion

Based on a careful comparison with the microscopic evolution in kinetic theory, we find that viscous hydrodynamics provides an accurate description of the space-time dynamics of high-energy high-power ion collisions if and only if the system is close enough to equilibrium, as given by The inverse Reynolds number is quantified. Clearly, this is not the case in the early stages of the collision, regardless of the ratio of shear viscosity to entropy density. where the system is highly anisotropic and the inhomogeneous longitudinal cooling cannot be properly described in conventional viscous hydrodynamics. Ignoring this effect leads to small deviations at the percentage level in the development of anisotropic transverse flow even at very small viscosities. However, for small enough viscosities, this effect can be compensated for by a local inhomogeneous scaling of the initial energy density profile, or by using a hybrid description where the energy momentum tensor after the initial kinetic evolution of the conditions It provides the initial for the next hydrodynamic stage. It is also conceivable that improved hydrodynamic theories, such as anisotropic hydrodynamics or hybrid schemes based on the corona core image, could further the practical limits by improving the far-from-equilibrium description, and it would be interesting to investigate this further in the future. Similarly, in very peripheral collisions or if the quark-gluon-plasma shear viscosity were significantly larger, the system would remain out of equilibrium for a significant part or even all of its space-time evolution, so that hydrodynamics only It becomes applicable at very late times, when transverse expansion is already very significant. Based on our analysis, we reasoned that if the damping exceeds values of three or four, a meaningful and accurate hydrodynamic description of the collective flow can be obtained. Since in our simplified kinetic description the non-equilibrium evolution is governed by a dimensionless quenching parameter, it is tempting to speculate on the implications of our findings for the theoretical description of small colliding systems. Based on experimental measurements of the transverse energy per unit velocity and theoretical estimates of the system size, we can deduce it for a value of quenching of about 0.7 not applicable in collisional systems. Interestingly, the case of collisions is more sensitive when the blackouts range from size 1.5 in minimal bias events to the limits of hydrodynamic application in high frequency events where size 2.7 can be reached. Unfortunately, however, the geometry of the initial state of collisions is now also limited, so that it becomes difficult to separate the effects of the geometry from those of the flow response. Nevertheless, the onset

of hydrodynamic behavior will also be investigated in collisions where large hadron collider energies, estimated quenches, range from 1.4 in peripheral events and 2.2 in intermediate central events to 3.1 in central events. As the geometry of collisions in pair colliders has become much more constrained, we expect such collisions to provide not only a critical test of the application of hydrodynamics to high-energy ion collisions, but also to the exciting region of non-equilibrium quantum chromodynamics between central and peripheral events. also penetrate.

REFERENCES

[1] D. A.Teaney,Viscous hydrodynamics and the quark gluon plasma
[2] H. Song, S. A. Bass, U. Heinz, T. Hirano, Phys. Rev. Lett. 106, 192301 (2011).
[3] H. Song, S. A. Bass, U. Heinz, T. Hirano, and C. Shen,Phys.Rev(2011)
[4] C. Gale, S. Jeon, and B. Schenke,INT.Phys. A 28 1340011 (2013)
[5] U. Heinz and R. Snellings,Annu. Rev.Nucl. part.Sci.63,123 (2013)
[6] M. Luzum and H. Petersen, J.Phys. G 41,063102 (2014.
[7] S. Jeon and U. Heinz, Int J. Mod. Phys. E 24,1520010 (2015)
[8] J. H. Putschke et al., arXiv:1903.07706
[9] D. Everett et al. (JETSCAPE Collaboration), Phys. Rev. C 145
[10] G. Nijs, W. van der Schee, Phys. Rev. C 103, 103, 054909 (2021)
[11] B. B. Abelev et al. (ALICE Collaboration), Phys. Rev. C 90
[12] M. Aaboud et al. (ATLAS Collaboration), Eur. Phys. J.C
[13] A. M. Sirunyan et al. (CMS Collaboration), Phys. Rev. Lett. 120, 092301 (2018)
[14] K. Dusling, W. Li, and B. Schenke,Int. J. Mod. Phys. E 25, 1630002 (2016)
[15] C. Loizides, Nucl.Phys. A956, 200 (2016)
[16] J. L. Nagle and W. A. Zajc, Annu. Rev. Nucl. Part. Sci. 68, 211 (2018).
[17] J. Berges, K. Boguslavski,S.Schlichting, Phys. Rev. D 89, 114007 (2014).
[18] J. Berges, K. Boguslavski, S. Schlichting, J. High Energy Phys. 05 (2014)
[19] M. P. Heller and M. Spalinski, Phys. Rev. Lett. 115, 072501(2015).
[20] M. Spaliński, Phys. Lett. B 776, 468 (2018).
[21] M. Strickland, J. Noronha, and G. S. Denicol, Phys. Rev. D97, 036020 (2018).
[22] M. Strickland, J. High Energy Phys. 12 (2018) 128.
[23] M. Spaliński, Phys. Lett. B 784, 21 (2018).
[24] G. Giacalone, A. Mazeliauskas, and S. Schlichting, Phys. Rev, 262301 (2019).
[25] A. Kurkela, W.. A. Wiedemann, Phys. Rev.Lett. 124, 102301 (2020).
[26] G. S. Denicol and J. Noronha, Phys. Rev. Lett. 124, 152301(2020).
[27] D. Almaalol, A. Kurkela, Phys. Rev. Lett. 125, 122302 (2020).
[28] M. P. Heller, R. Jefferson, M. Svensson, Phys. Rev. Lett. 125, 132301 (2020).
[29] X. Du and S. Schlichting, Phys. Rev. Lett. 127, 122301 (2021).
[30] J.-P. Blaizot and L. Yan, Phys. Rev. C 104, 055201 (2021).
[31] C. Chattopadhyay, S. Jaiswal, L.,and S. Pal, Phys. Lett, 136820 (2022)
[32] X. Du, M. P. Heller, S. Schlichting, and V. Svensson, Phys. Rev, 014016 (2022).
[33] G. S. Denicol, U. W. Heinz, M. Martinez, J. Noronha, and
[34] M. Strickland, Phys. Rev. D 90, 125026 (2014).
[35] A. Kurkela, U. A. Wiedemann, and B. Wu, Eur. Phys. J. C79, 965 (2019).
[36] A. Kurkela, S. F. Taghavi, and B. Wu, Phys. Lett. B 135901 (2020).
[37] V. E. Ambrus, S. Schlichting, and C. Werthmann, arXiv: 2211.14379.
[38] V. E. Ambruş, S. Schlichting, and C. Werthmann, Phys. Rev. (2022).

[39] N. Borghini, M. Borrell, N. Schlichting, Phys. Rev. C 107, 034905 (2023).
[40] J. I. Kapusta, Phys. Rev. C 21, 1301 (1980).
[41] H. Petersen, J. Steinheimer, M. Bleicher, J. Phys. G 36, 055104 (2009).
[42] P. Huovinen and H. Petersen, Eur. Phys. J. A 48, 171 (2012).
[43] I. Karpenko, P. Huovinen, and M. Bleicher, Comput. Phys..
[44] I. Müller, Z. Phys. 198, 329 (1967).
[45] W. Israel and J. M. Stewart, Ann. Phys. (N.Y.) 118, 341 (1979).
[46] H. Heiselberg and A.-M. Levy, Phys. Rev. C 59, 2716 (1999).
[47] N. Borghini and C. Gombeaud, Eur. Phys. J. C 71, 1612 (2011).
[48] P. Romatschke, Eur. Phys. J. C 78, 636 (2018).
[49] A. Kurkela, U. A. Wiedemann, and B. Wu, Phys. (2018).
[50] N. Borghini, S. Feld, and N. Kersting, Eur. Phys. J. C 78, 832 (2018).
[51] A. Kurkela, A. Mazeliauskas, and R. Törnkvist, J. High (2016)
[52] B. Bachmann, N. Borghini, N. Feld, and H. Roch, Phys. J. C 83, 114 (2023).
[53] J. E. Bernhard, J. S. Moreland, and S. A. Bass, Phys. (2019)
[54] J. D. Bjorken, Phys. Rev. D 27, 140 (1983).
[55] J. Jankowski, S. Kamata, M. Martinez, Phys. Rev. D 104, 074012 (2021). See Supplemental Material at http://link.aps.org/ supplemental/10.1103/PhysRevLett.130.152301 for additional results regarding radial flow and plasma cooling, discussion of an initial condition closer to common practice, and a disclosure of how we obtained opacity estimates. This material includes Refs.
[56] See Supplemental Material at http://link.aps.org/ supplemental/10.1103/PhysRevLett.130.152301 for additional results regarding radial flow and plasma cooling, discussion of an initial condition closer to common practice, and a disclosure of how we obtained opacity estimates.
[57] See Supplemental Material at http://link.aps.org/ supplemental/10.1103/PhysRevLett.130.152301 for additional results regarding radial flow and plasma cooling, discussion of an initial condition closer to common practice, and a disclosure of how we obtained opacity estimates.
[58] See Supplemental Material at http://link.aps.org/ supplemental/10.1103/PhysRevLett.130.152301 for additional results regarding radial flow and plasma cooling, discussion of an initial condition closer to common practice, and a disclosure of how we obtained opacity estimates.
[59] B. B. Abelev et al. (ALICE Collaboration), Phys. Lett. B (2013)
[60] B. B. Abelev et al. (ALICE Collaboration), arXiv:2204. 10210.
[61] G. Nijs and W. van der Schee, Phys. Rev. C 106, 044903 (2022)
[62] G. S. Denicol, H. Niemi, E. Molnar, and D. H. Rischke, 91, 039902(E) (2015).
[63] S. Floerchinger and U. A. Wiedemann, J. High Energy Phys. 11 (2011) 100.
[64] H. Niemi and G. S. Denicol, arXiv:1404.7327.
[65] M. Martinez and M. Strickland, Nucl. Phys. A848, 183 (2010).
[66] W. Florkowski and R. Ryblewski, Phys. Rev. C 83, 034907 (2011).
[67] W. Florkowski, R. Ryblewski, and M. Strickland, Phys. 024903 (2013).
[68] M. Martinez, R. Ryblewski, and M. Strickland, Phys. Rev. C (2012)
[69] M. McNelis, D. Bazow, and U. Heinz, Comput. Phys. Commun. (2021).
[70] K. Werner, Phys. Rev. Lett. 98, 152301 (2007).
[71] Y. Kanakubo, Y. Tachibana, and T. Hirano, Phys. Rev. C (2020)
[72] S. Demirci, T. Lappi, and S. Schlichting, Phys. Rev. D 106, 074025 (2022).
[73] B. Schenke and R. Venugopalan, Phys. Rev. Lett. 113, 102301 (2014).

[74] Fazelpour, F., Bakhshayesh, A., Alimohammadi, R. et al. An assessment of reducing energy consumption for optimizing building design in various climatic conditions. Int J Energy Environ Eng 13, 319–329 (2022). https://doi.org/10.1007/s40095-021-00461-6

[75] Iranfar A, Saraei A. Numerical study of nanoencapsulated phase change material inside double pipe heat exchanger. Heat Transfer—Asian Res. 2019; 48: 3466–3476. https://doi.org/10.1002/htj.21549

[76] Riyahi, N., Saraei, A., Vahdat Azad, A. et al. Energy analysis and optimization of a hybrid system of reverse osmosis desalination system and solar power plant (case study: Kish Island). Int J Energy Environ Eng 13, 67–75 (2022). https://doi.org/10.1007/s40095-021-00418-9